



Operation of
Airmodus PSM

J. Kangasluoma et al.

This discussion paper is/has been under review for the journal Atmospheric Measurement Techniques (AMT). Please refer to the corresponding final paper in AMT if available.

Operation of the Airmodus A11 nano Condensation Nucleus Counter at various inlet pressures, various operation temperatures and design of a new inlet system

J. Kangasluoma¹, A. Franchin¹, J. Duplissy¹, L. Ahonen¹, F. Korhonen¹, M. Attoui², J. Mikkilä¹, K. Lehtipalo¹, J. Vanhanen³, M. Kulmala¹, and T. Petäjä¹

¹Department of Physics, P.O. Box 64, 00014, University of Helsinki, Helsinki, Finland

²LISA, University Paris Est Creteil, 94010, Creteil, France

³Airmodus Ltd., Pietari Kalminkatu 1 F 1, 00560 Helsinki, Finland

Received: 12 May 2015 – Accepted: 15 June 2015 – Published: 10 August 2015

Correspondence to: J. Kangasluoma (juha.kangasluoma@helsinki.fi)

Published by Copernicus Publications on behalf of the European Geosciences Union.

Title Page

Abstract

Introduction

Conclusions

References

Tables

Figures



Back

Close

Full Screen / Esc

Printer-friendly Version

Interactive Discussion



Abstract

Measuring sub-3 nm particles outside of controlled laboratory conditions is a challenging task, as many of the instruments are operated at their limits and are subjected to changing ambient conditions. In this study, we advance the current understanding on the operation of Airmodus A11 nano Condensation Nucleus Counter (nCNC), which consists of a A10 Particle Size Magnifier (PSM) and A20 condensation particle counter (CPC). We explore the effect of the inlet line pressure on the measured particle concentration. We identify two different regions inside the instrument where supersaturation of working fluid can take place. We show the possibility of varying the cut-off of the instrument from 1 to 6 nm, a wider size range than the one usually covered by the PSM. We also present a new inlet system, which allows automated measurements of the background, minimizes the diffusion losses in the sampling line and is equipped with an electrostatic filter to remove ions. Finally, our view of the guidelines for optimal use of the Airmodus nCNC are provided.

1 Introduction

In suitable atmospheric conditions, gases and vapors form small clusters and nanoparticles, some of which can subsequently grow into large enough particles to affect climate by influencing cloud formation and by scattering sunlight (Kulmala et al., 2004; Kerminen et al., 2012). With the development of new particle counters (Vanhanen et al., 2011; Jiang et al., 2011; Sipila et al., 2009; Wimmer et al., 2013), measurements of new particle formation have been extended to molecular sizes. Based on laboratory verifications, these new particle counters are able to activate and detect large molecules and molecular clusters. They are deployed in field experiments, on the assumption that laboratory calibrations are representative of field conditions.

A general method to detect small nanoparticles is to bring the particles into a region of supersaturated gas, which will condense onto the surface of the particles. Subse-

AMTD

8, 8483–8508, 2015

Operation of Airmodus PSM

J. Kangasluoma et al.

Title Page

Abstract

Introduction

Conclusions

References

Tables

Figures



Back

Close

Full Screen / Esc

Printer-friendly Version

Interactive Discussion



Operation of Airmodus PSM

J. Kangasluoma et al.

Title Page

Abstract

Introduction

Conclusions

References

Tables

Figures

◀

▶

◀

▶

Back

Close

Full Screen / Esc

Printer-friendly Version

Interactive Discussion



tions inside the instrument, making it possible to measure size distributions of 1–2 nm particles. Vanhanen et al. (2011) report theoretical prediction of maximum supersaturation at a mixing ratio of 0.1, whereas their experiments showed that supersaturation continued to increase at mixing ratios higher than 0.1. The mixing ratio is defined as:

$$(Q_{\text{saturator}} / (Q_{\text{aerosol}} + Q_{\text{saturator}})).$$

In this technical study, we concentrate on the challenges related to the effect of pressure on the flows of the PSM and to the heterogeneous nucleation of DEG onto the sampled particles. We identify two different supersaturation fields inside the PSM and show that the PSM could be used to measure size distributions between 1 and 6 nm. The increased measurement capability is achieved by scanning the growth tube temperature inside the PSM at constant flows, eliminating the need for mass flow meters. We also illustrate how to select and understand suitable temperatures and flows inside the PSM to achieve optimal performance. The temperatures and conditions used in this work do not apply to every PSM or to every experiment. Variations in the calibrations of temperature sensors, in particle composition and in the relative humidity of the sample flow might affect the PSM calibration. Thus, we only want to illustrate the problems and give a qualitative solution, which users should quantify for their own experiments. Finally, we describe a sampling inlet line that is found to be suitable for long term field measurements.

2 Experimental

First we define the terms used in the experiments. The total detection efficiency of A11 system is given by equation

$$\varepsilon_{A11} = \varepsilon_{\text{PPSM}} \cdot \varepsilon_{\text{aPSM}} \cdot \varepsilon_{\text{pCPC}} \cdot \varepsilon_{\text{aCPC}} \cdot \varepsilon_{\text{cCPC}} \quad (1)$$

where $\varepsilon_{\text{PPSM}}$ is penetration through the PSM, $\varepsilon_{\text{aPSM}}$ is activation efficiency of the PSM, $\varepsilon_{\text{pCPC}}$ is penetration through CPC and the sampling line, $\varepsilon_{\text{aCPC}}$ is activation efficiency

Operation of Airmodus PSM

J. Kangasluoma et al.

Title Page

Abstract

Introduction

Conclusions

References

Tables

Figures

◀

▶

◀

▶

Back

Close

Full Screen / Esc

Printer-friendly Version

Interactive Discussion



of the CPC and ε_{CPC} is counting efficiency of the CPC. Usually ε_{A11} is called “detection efficiency” of the A11, which is the term we use here. In our experiments when a conventional A11 calibration is conducted, the concentration detected by the A11 is compared to a concentration measured by an aerosol electrometer with identical losses in the sampling line, and ε_{A11} is directly obtained. From here, in our text “PSM” refers to the combination of the A10 PSM and A20 CPC.

2.1 The effect of under pressure

We probed the pressure dependency of DEG heterogeneous nucleation inside the PSM by strangling the sampling flow with a needle valve upstream of the PSM. To simulate PSM measurements at higher altitudes we measured down to 50 kPa, which corresponds approximately to 4000 m in altitude. To obtain the pressure dependency of the inlet flow of the PSM, two TSI mass flow meters (model 4043) were located upstream and downstream of a needle valve, which was placed in the inlet line of the PSM. Additionally, the flows were calculated by taking into account the pressure dependency of the mass flow controllers inside the PSM. The mass flows were calculated by Q/p , where Q is volume flow and p is pressure in bars. The inlet flow of the CPC was assumed to be constant since it is controlled with a critical orifice, which keeps the volume flow constant. From these three flows the inlet flow at normal pressure is given by

$$Q_{\text{inlet}} = Q_{\text{excess}} + Q_{\text{CPC}} - Q_{\text{saturator}}, \quad (2)$$

and the inlet flow at low pressure is given by

$$Q_{\text{inlet_low_pressure}} = Q_{\text{excess}}/p + Q_{\text{CPC}} - Q_{\text{saturator}}/p \quad (3)$$

To probe the effect of pressure on the detected concentrations, we generated 50 nm ammonium sulfate particles with an atomizer and a Hauke-type DMA. The pressures inside the electrometer, the PSM and the PSM saturator were adjusted with the needle

Operation of Airmodus PSM

J. Kangasluoma et al.

Title Page

Abstract

Introduction

Conclusions

References

Tables

Figures



Back

Close

Full Screen / Esc

Printer-friendly Version

Interactive Discussion



valve in the sampling line by strangling the flow (Fig. 2a). A tube, branching off the sampling line, was attached to the fill bottle connector to equilibrate the pressure in the PSM saturator. The fill bottle was not used in our experiments, since higher ambient pressure squeezes the bottle when the sampling line is at low pressure. The concentration measured by the PSM was compared to the electrometer at pressures from 50 to 100 kPa. To separate the pressure dependency of the PSM and the CPC, similar experiments were conducted on the CPC alone.

The effect of pressure on the 50 % cut-off (diameter where 50 % of the particles are detected) diameter of the PSM was measured at 60, 80 and 100 kPa by generating negative tungsten oxide particles (Kangasluoma et al., 2015) from 1 to 3 nm (Fig. 2a).

2.2 Operation temperatures

The PSM can be operated in two modes, in laminar mode or in mixing mode. We define these modes based on where the activation of the particles is taking place. If the highest supersaturation is in the mixing zone, the PSM is operated in mixing mode. If the highest supersaturation is inside the growth tube, the PSM is operated in laminar mode. By changing the temperature set points in the inlet, saturator and growth tube, it is possible to determine where the highest supersaturation is. An example of a temperature setting that would allow the PSM to operate in laminar mode is: saturator at 85 °C, inlet at 35 °C and growth tube at 5 °C. To operate the PSM in mixing mode, a possible temperature setting is: saturator at 76 °C, inlet at 0 °C and growth tube at 40 °C. With these temperature settings, different sizes (from 1.1 to 2.4 nm) of hydrogen sulfate particles were selected with a DMA and sent to the PSM, and the saturator flow rate was scanned from 0.1 to 1 Lmin⁻¹ (Fig. 2b). This is the conventional PSM calibration.

Mixing-type activation can happen, for example, when the sample air is very cold. In this case, a large temperature difference between the inlet and the saturator is achieved. Interestingly, mixing-type activation can happen even if the PSM is set to operate in laminar mode. In some ambient conditions, mixing-type activation is unin-

**Operation of
Airmodus PSM**

J. Kangasluoma et al.

Title Page

Abstract

Introduction

Conclusions

References

Tables

Figures



Back

Close

Full Screen / Esc

Printer-friendly Version

Interactive Discussion



entionally reached in the PSM. When that happens, the supersaturation experienced by the entering particles might not be monotonically increasing with the increasing saturator flow, making it difficult to invert the data. We performed an experiment that demonstrates the problem: THABr monomer (Ude and de la Mora, 2005) was fed into the PSM at room temperature (23 °C), and the inlet temperature was varied from 0 to 40 °C to simulate a strongly varying inlet flow temperature. The saturator was set to 82 °C and the growth tube to 1 °C.

The activation efficiency is governed by the temperature difference inside the PSM. Therefore, we tested the maximum detectable size range by scanning the growth tube temperature, instead of by scanning the saturator flow. In the experiments, the growth tube was set to 1 °C and other temperatures so that the detection efficiency for 1 nm particles is 30 %. Thereafter we increased the growth tube temperature up to 40 °C to find out the maximum detectable size.

2.3 Sampling line

The sampling line system consists of one blower and two three-way-valves, which control the direction of the air flow (Fig. 3a) and a core sampling probe (Fig. 3b). By switching the valves, the air flow can be directed to the core sampling piece in either direction. If the air is sucked from the core sampling, it increases the inlet flow and minimizes the diffusion losses. If the air is pushed towards the core sampling, the background of the PSM can be measured, since the instrument is fed with a portion of the extra aerosol-free air flow. The sampling line also contains an automatic on/off electric field, which filters the smallest incoming ions, allowing only neutral particles to be detected. The valve switching is made automatic so that in the field the zero can be measured at given time intervals for given time period, and the ion filter can be switched on/off at given time interval. The sampling line was characterized for the transmission by generating 1.1 to 6.5 nm tungsten oxide particles with the instrumental setup shown in Fig. 2c. Using the same aerosol, the ion filtering was tested by switching the electric field on and off.

3 Results and discussion

3.1 The effect of under pressure

The measured and modelled PSM flows are presented in Fig. 4 as a function of pressure. The saturator mass flow and the excess mass flow control the inlet flow of the PSM. The measured inlet flows are well reproduced by the calculated flows.

As the absolute changes in the saturator and excess flows are different, the dilution correction ($Q_{\text{inlet}}/(Q_{\text{inlet}} + Q_{\text{saturator}})$) in the PSM mixing zone varies, changing the detected concentration. In addition, the counting efficiency of the CPC is lower at lower pressure, probably due to changing flow dynamics or final particle size in the optics.

The detection efficiency for a 50 nm ammonium sulfate particles is presented in Fig. 5 at varying pressure for the A11 system. The Figure presents detection efficiency, which is scaled to 1 to show effects caused only due to under pressure. The red data are corrected with the calculated dilution correction, the black data are corrected for the CPC under-counting and the green data are corrected for both effects. The CPC counting efficiency correction was obtained by measuring the counting efficiency of the CPC without the PSM separately against the electrometer. For example, at a pressure of 60 kPa the dilution correction, compared to that at 100 kPa, increases by 3.5%, due to changing mass flows, as shown in Fig. 5. The CPC undercounts by approximately 10%, giving a total underestimation of 13.5% of the detected concentration at 60 kPa.

Almost no correction is needed at 80 kPa or higher. It is important to note that in low pressure experiments, as the CPC volume flow decreases with decreasing pressure the aerosol volume concentration in the optics also decreases. For example, at 50 kPa the observed concentration is half of the observed concentration that is measured at 100 kPa. In Fig. 5 this correction is applied.

The measured cut-offs at PSM settings $T_{\text{sat}} = 75^\circ\text{C}$, $T_{\text{inlet}} = 35^\circ\text{C}$ and $T_{\text{gt}} = 4^\circ\text{C}$ are presented in Fig. 6 at 60, 80 and 100 kPa. With these settings, the cut-off diameters are 1.60, 1.60 and 1.55 nm respectively. The change in the cut-off can be explained by the changing dilution factor, which increases the supersaturation slightly at lower pressure,

Title Page

Abstract

Introduction

Conclusions

References

Tables

Figures



Back

Close

Full Screen / Esc

Printer-friendly Version

Interactive Discussion



compared to ambient pressure. The change is rather small given the uncertainties in the cut-off, which are due to the particle chemical composition (Kangasluoma et al., 2014).

3.2 Operation temperatures

In our study we confirm the calculation of Vanhanen et al. (2011) for the peak supersaturation at mixing ratio 0.1. The PSM calibration in mixing mode is presented in Fig. 7 and, for comparison, a laminar mode calibration is presented in Fig. 8. The temperature settings mentioned above in mixing mode lead to onset supersaturation of homogeneous nucleation at saturator flow 0.3–0.7 L min⁻¹. As calculated by Vanhanen et al. (2011), the maximum supersaturation should occur at a mixing ratio of approximately 0.1 and get lower at higher mixing ratios. Mixing ratio 0.1 corresponds to a saturator flow 0.28 L min⁻¹ and is approximately reproduced by the experiments, as the maximum detection efficiency for the smallest particles is observed at saturator flows approximately 0.3 L min⁻¹. The lower supersaturation at flows > 0.3 L min⁻¹ is also observed. However, with particles > 1.4 nm the maximum activation efficiency seems to shift towards larger saturator flows for reasons that we cannot yet explain. If the PSM is operated in mixing mode, the maximum detection for particles smaller than 1.5 nm is rather low. Moreover, the shape of the activation curve as a function of saturator flow is changing. For these reasons we suggest keeping the PSM operation in laminar mode for easier inversion of data, as presented in Lehtipalo et al. (2014).

To activate the THABr positive monomer with high efficiency using DEG, a supersaturation exceeding that of homogeneous nucleation is required. It is important to note that high saturator temperatures lead to a high temperature difference between the saturator and the inlet when the PSM is operated in laminar mode. This high temperature difference can enable mixing-type activation in the mixing chamber, as shown in Fig. 9 (high concentrations at saturator flow 0.3 L min⁻¹). The lower the inlet temperature, the higher the background concentration generated in the mixing region becomes. Notably, the inlet temperature influences the temperature and the supersaturation in the growth

Operation of Airmodus PSM

J. Kangasluoma et al.

Title Page

Abstract

Introduction

Conclusions

References

Tables

Figures



Back

Close

Full Screen / Esc

Printer-friendly Version

Interactive Discussion



**Operation of
Airmodus PSM**

J. Kangasluoma et al.

Title Page

Abstract

Introduction

Conclusions

References

Tables

Figures



Back

Close

Full Screen / Esc

Printer-friendly Version

Interactive Discussion



tube. In particular, the activation efficiency increases in the growth tube with lower inlet temperatures. At a saturator flow 1 L min^{-1} , we observe an increase in detection efficiency from 10 to 50 %, resulting in a decrease in the cut-off diameter of approximately 0.2 nm. The illustrated background concentration is likely to appear only if the PSM is operated at supersaturations high enough to produce homogeneous nucleation of DEG, which is required to detect some organic $< 2 \text{ nm}$ particles. Based on these experiments, we suggest keeping the inlet temperature as high as possible, keeping the growth tube temperature as low as possible, and adjusting the supersaturation by changing the saturator temperature. This way the temperature difference between the inlet and the saturator is minimized. The background concentration at a saturator flow of 0.3 L min^{-1} seems to be independent from the concentration of the incoming sample, which we have not observed at saturator flow 1 L min^{-1} . It suggests that the homogeneously formed droplets form before the mixing region and do not activate any particles. On the other hand, at a saturator flow of 1 L min^{-1} (laminar type activation) the homogeneous nucleation inside the instrument is usually a good indication of activation efficiency (Jiang et al., 2011).

We conducted a calibration to investigate the change in supersaturation inside the PSM by varying the growth tube temperature instead of by changing the flow settings of the saturator (Fig. 10). We found that the maximum detectable size is approximately 6 nm, while preserving high sensitivity to particles as small as 1 nm. Thus, scanning the growth tube temperature would allow the measurement of a wider scan range without the change of flows necessary for scanning the saturator flow. With the current hardware, we estimate the time resolution of the temperature scan to be around 7 to 10 min.

3.3 Sampling inlet

By adding 5 L min^{-1} as a bypass flow to the PSM inlet flow and sub-sampling from the centerline of the long tube, the PSM can sample 40 cm away from the inlet without losing sampling efficiency for the smallest particles (Fig. 11). This is ideal when using

**Operation of
Airmodus PSM**

J. Kangasluoma et al.

Title Page

Abstract

Introduction

Conclusions

References

Tables

Figures



Back

Close

Full Screen / Esc

Printer-friendly Version

Interactive Discussion



the PSM in the field. Diffusion to the walls is most efficient close to the tube walls, and when sampling from the middle of the 10 mm tube, only a fraction of the sample which has not lost particles due to diffusion is sampled. Doubling the sampling line length to 80 cm increases the losses as the particles have time to diffuse away from the middle of the flow. However, the inlet allows the sampling efficiency to increase by a factor of 1.5 to 2 compared to a penetration calculated using the Gormley and Kennedy equation at 2.5 L min^{-1} and through an 80 cm line. For our calculations, we used an inlet flow of 2.5 L min^{-1} , to simulate the case when no core sampling inlet is utilized and the inlet line is a straight tube with no additional flow. When the electric field is switched on/off, it is possible to measure the charged and neutral fraction of the sample by complete removal of ions larger than 4.5 nm. By varying the electric field, the size of the biggest removed ion could be varied (not shown). In the experiments, the voltage difference was 1300 V.

4 Conclusions

In the current study, we have explored the characteristics of the PSM instrument in challenging conditions. The challenges and suggested solutions are listed in Table 1. Our results show that, when operated at low pressure, the PSM-CPC system underestimates the real aerosol number concentration due to changes in the mass flows inside the PSM and due to CPC undercounting. We show that at a given flow and temperature condition the PSM behaves as a laminar-type CPC, but can be converted into a mixing-type CPC. Understanding how supersaturation in the PSM behaves, we reproduced a problem observed in some field experiments, where mixing-type activation interferes with the laminar activation, an interference that can make it difficult to invert the data and to retrieve size information in the range of 1 to 2 nm. For optimal operation, we suggest keeping the growth tube temperature as low as needed and the inlet temperature as high as possible, to reduce the saturator temperature and ultimately minimize the temperature difference between the inlet and saturator. We showed that

by scanning the growth tube temperature, the PSM can potentially measure size distributions up to 6 nm. Finally, with a proper design of the sampling inlet, it is possible to measure automated background and charged fraction, and to achieve a transmission efficiency close to 100 % for 40 cm of inlet line.

5 *Acknowledgements.* This work was partly funded by European Research Council (ATMNU-CLE, 227463), Academy of Finland (Center of Excellence Program projects 1118615 and 139656), Nordic Center for Excellence (CRAICC), European Commission seventh Framework program (ACTRIS, contract no 262254; PEGASOS, contract no 265148), Office of Science (BER), and U.S. Department of Energy (The Biogenic Aerosols – Effects of Clouds and Climate, BAECC).

References

Iida, K., Stolzenburg, M. R., and McMurry, P. H.: Effect of working fluid on sub-2 nm particle detection with a laminar flow ultrafine condensation particle counter, *Aerosol Sci. Tech.*, 43, 81–96, doi:10.1080/02786820802488194, 2009.

15 Jiang, J. K., Chen, M. D., Kuang, C. A., Attoui, M., and McMurry, P. H.: Electrical mobility spectrometer using a diethylene glycol condensation particle counter for measurement of aerosol size distributions down to 1 nm, *Aerosol Sci. Tech.*, 45, 510–521, doi:10.1080/02786826.2010.547538, 2011.

20 Kangasluoma, J., Junninen, H., Lehtipalo, K., Mikkilä, J., Vanhanen, J., Attoui, M., Sipilä, M., Worsnop, D., Kulmala, M., and Petäjä, T.: Remarks on ion generation for CPC detection efficiency studies in sub-3-nm size range, *Aerosol Sci. Tech.*, 47, 556–563, doi:10.1080/02786826.2013.773393, 2013.

25 Kangasluoma, J., Kuang, C., Wimmer, D., Rissanen, M. P., Lehtipalo, K., Ehn, M., Worsnop, D. R., Wang, J., Kulmala, M., and Petäjä, T.: Sub-3 nm particle size and composition dependent response of a nano-CPC battery, *Atmos. Meas. Tech.*, 7, 689–700, doi:10.5194/amt-7-689-2014, 2014.

Kangasluoma, J., Attoui, M., Junninen, H., Lehtipalo, K., Samodurov, A., Korhonen, F., Sarnela, N., Schmidt-Ott, A., Worsnop, D., Kulmala, M., and Petäjä, T.: Sizing of neutral sub 3 nm

Operation of Airmodus PSM

J. Kangasluoma et al.

Title Page

Abstract

Introduction

Conclusions

References

Tables

Figures



Back

Close

Full Screen / Esc

Printer-friendly Version

Interactive Discussion



**Operation of
Airmodus PSM**

J. Kangasluoma et al.

Title Page

Abstract

Introduction

Conclusions

References

Tables

Figures



Back

Close

Full Screen / Esc

Printer-friendly Version

Interactive Discussion



tungsten oxide clusters using Airmodus Particle Size Magnifier, *J. Aerosol. Sci.*, 87, 53–62, 2015.

Kerminen, V.-M., Paramonov, M., Anttila, T., Riipinen, I., Fountoukis, C., Korhonen, H., Asmi, E., Laakso, L., Lihavainen, H., Swietlicki, E., Svenningsson, B., Asmi, A., Pandis, S. N., Kulmala, M., and Petäjä, T.: Cloud condensation nuclei production associated with atmospheric nucleation: a synthesis based on existing literature and new results, *Atmos. Chem. Phys.*, 12, 12037–12059, doi:10.5194/acp-12-12037-2012, 2012.

Kulmala, M., Laakso, L., Lehtinen, K. E. J., Riipinen, I., Dal Maso, M., Anttila, T., Kerminen, V.-M., Hörrak, U., Vana, M., and Tammet, H.: Initial steps of aerosol growth, *Atmos. Chem. Phys.*, 4, 2553–2560, doi:10.5194/acp-4-2553-2004, 2004.

Lehtipalo, K., Leppä, J., Kontkanen, J., Kangasluoma, J., Franchin, A., Wimmer, D., Schobesberger, S., Junninen, H., Petaja, T., Sipila, M., Mikkilä, J., Vanhanen, J., Worsnop, D. R., and Kulmala, M.: Methods for determining particle size distribution and growth rates between 1 and 3 nm using the Particle Size Magnifier, *Boreal Environ. Res.*, 19, 215–236, 2014.

Saros, M. T., Weber, R. J., Marti, J. J., and McMurry, P. H.: Ultrafine aerosol measurement using a condensation nucleus counter with pulse height analysis, *Aerosol Sci. Tech.*, 25, 200–213, doi:10.1080/02786829608965391, 1996.

Sipila, M., Lehtipalo, K., Attoui, M., Neitola, K., Petaja, T., Aalto, P. P., O'Dowd, C. D., and Kulmala, M.: Laboratory verification of PH-CPC's ability to monitor atmospheric sub-3 nm clusters, *Aerosol Sci. Tech.*, 43, 126–135, doi:10.1080/02786820802506227, 2009.

Ude, S. and de la Mora, J. F.: Molecular monodisperse mobility and mass standards from electrosprays of tetra-alkyl ammonium halides, *J. Aerosol Sci.*, 36, 1224–1237, doi:10.1016/j.jaerosci.2005.02.009, 2005.

Vanhanen, J., Mikkilä, J., Lehtipalo, K., Sipila, M., Manninen, H. E., Siivola, E., Petaja, T., and Kulmala, M.: Particle size magnifier for nano-CN detection, *Aerosol Sci. Tech.*, 45, 533–542, doi:10.1080/02786826.2010.547889, 2011.

Wimmer, D., Lehtipalo, K., Franchin, A., Kangasluoma, J., Kreissl, F., Kürten, A., Kupc, A., Metzger, A., Mikkilä, J., Petäjä, T., Riccobono, F., Vanhanen, J., Kulmala, M., and Curtius, J.: Performance of diethylene glycol-based particle counters in the sub-3 nm size range, *Atmos. Meas. Tech.*, 6, 1793–1804, doi:10.5194/amt-6-1793-2013, 2013.

Operation of Airmodus PSM

J. Kangasluoma et al.

Title Page

Abstract

Introduction

Conclusions

References

Tables

Figures



Back

Close

Full Screen / Esc

Printer-friendly Version

Interactive Discussion



Table 1. Brief compilation of challenges and solutions explored in this study.

Challenge	Solution
Varying inlet pressure	Depending on application, change in the cut-off can be neglected. Total concentration needs to be corrected with the mass-volume flow correction and CPC undercounting if pressure is smaller than 80 kPa.
M-shaped scans in field measurements	Caused by homogeneous/heterogeneous nucleation occurring in the mixing zone instead of the growth tube. Decrease growth tube temperature to minimum and maximize inlet temperature to minimize dT between the inlet and saturator. Adjust saturator for suitable activation efficiency.
Low penetration of small particles in the sampling line	Core sampling inlet with bypass flow, automated ion filter and background measurement.

**Operation of
Airmodus PSM**

J. Kangasluoma et al.

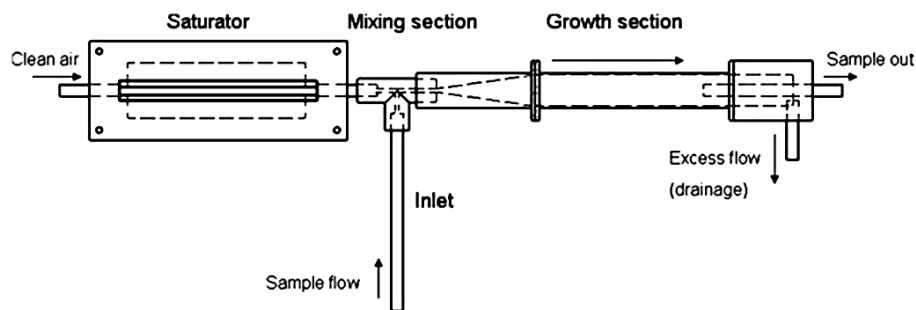


Figure 1. A schematic figure of the Particle Size Magnifier (PSM) (first published in Vanhanen et al., 2011).

Title Page

Abstract

Introduction

Conclusions

References

Tables

Figures

◀

▶

◀

▶

Back

Close

Full Screen / Esc

Printer-friendly Version

Interactive Discussion



Operation of Airmodus PSM

J. Kangasluoma et al.

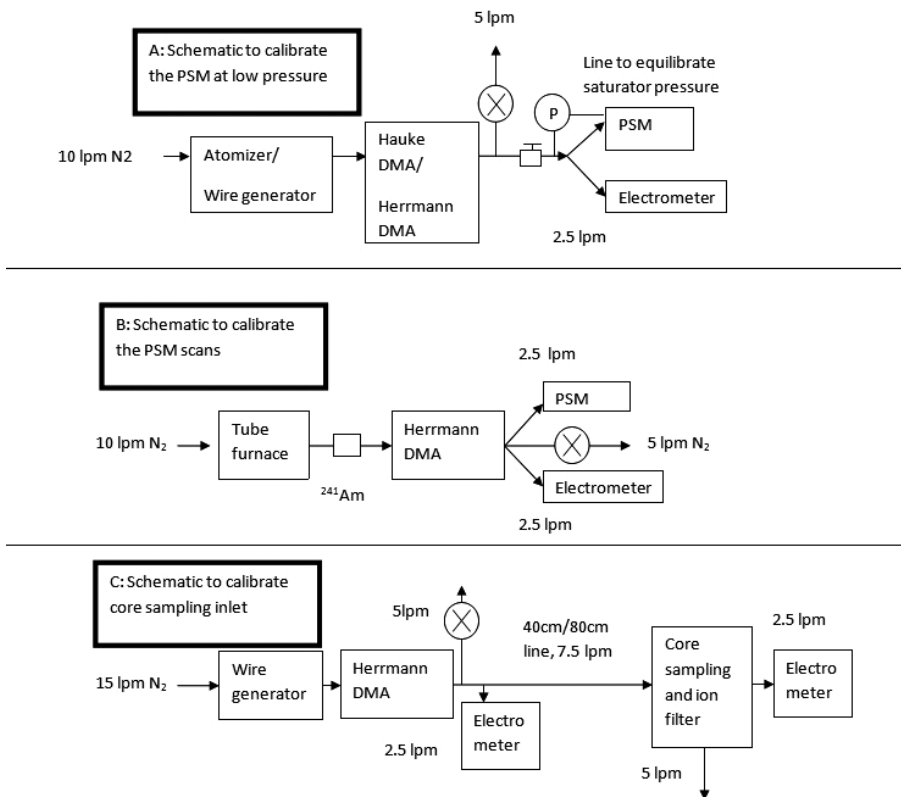


Figure 2. The utilized experimental setups.

Title Page	
Abstract	Introduction
Conclusions	References
Tables	Figures
◀	▶
◀	▶
Back	Close
Full Screen / Esc	
Printer-friendly Version	
Interactive Discussion	



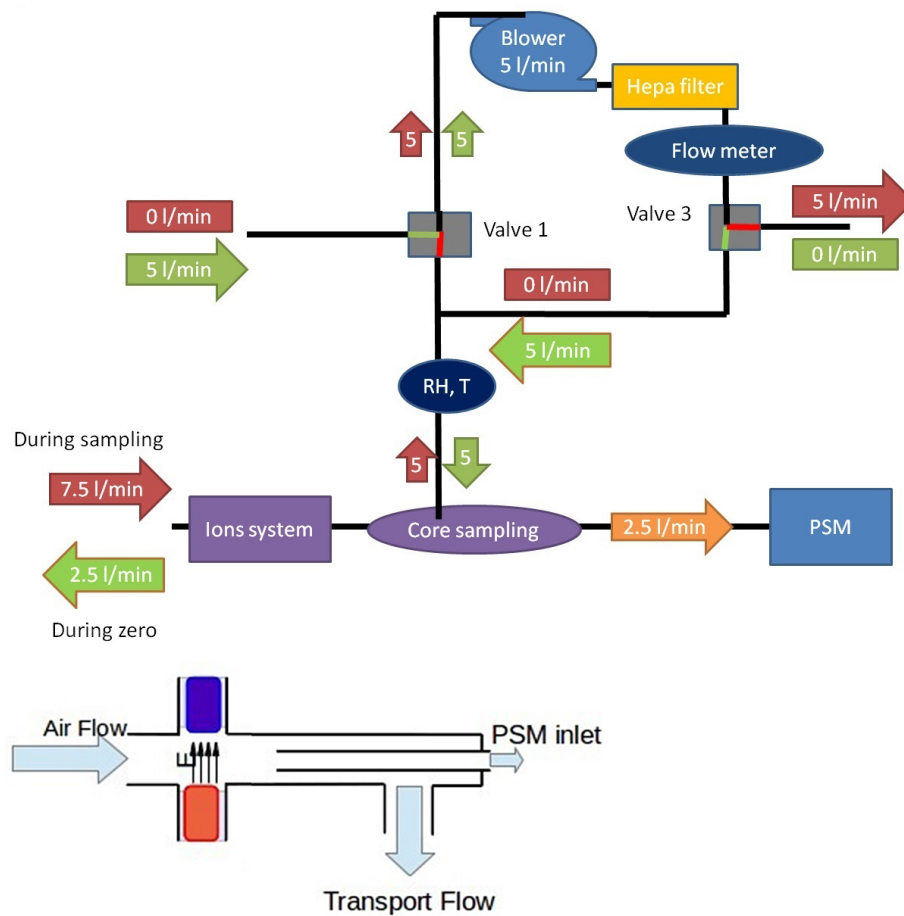


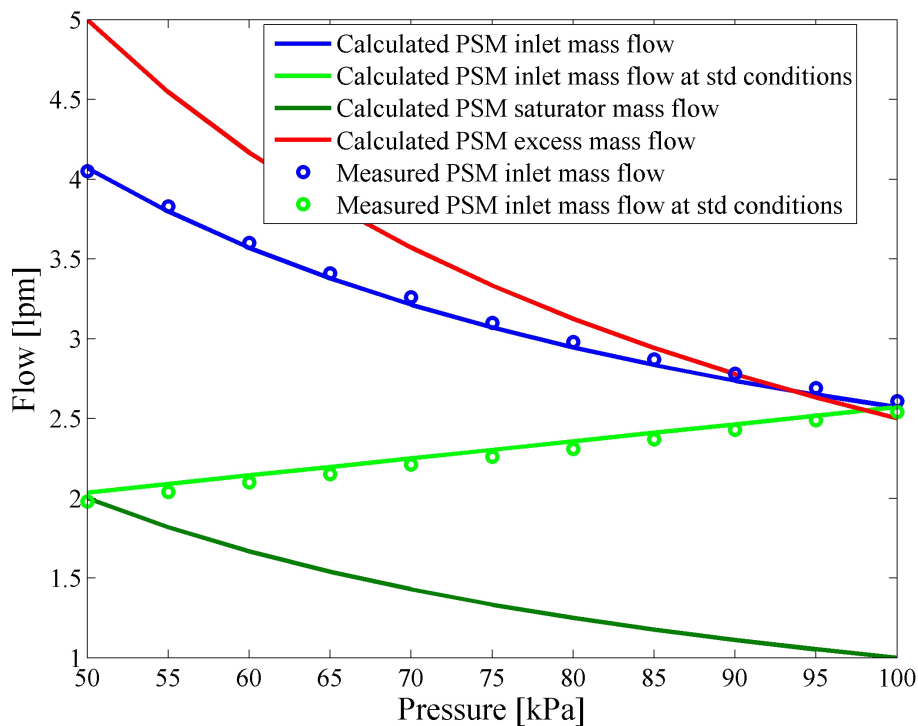
Figure 3. Schematic of the sampling line.

Title Page	
Abstract	Introduction
Conclusions	References
Tables	Figures
◀	▶
◀	▶
Back	Close
Full Screen / Esc	
Printer-friendly Version	
Interactive Discussion	



**Operation of
Airmodus PSM**

J. Kangasluoma et al.

**Figure 4.** The change in the mass flows inside the PSM due to changing inlet pressure.

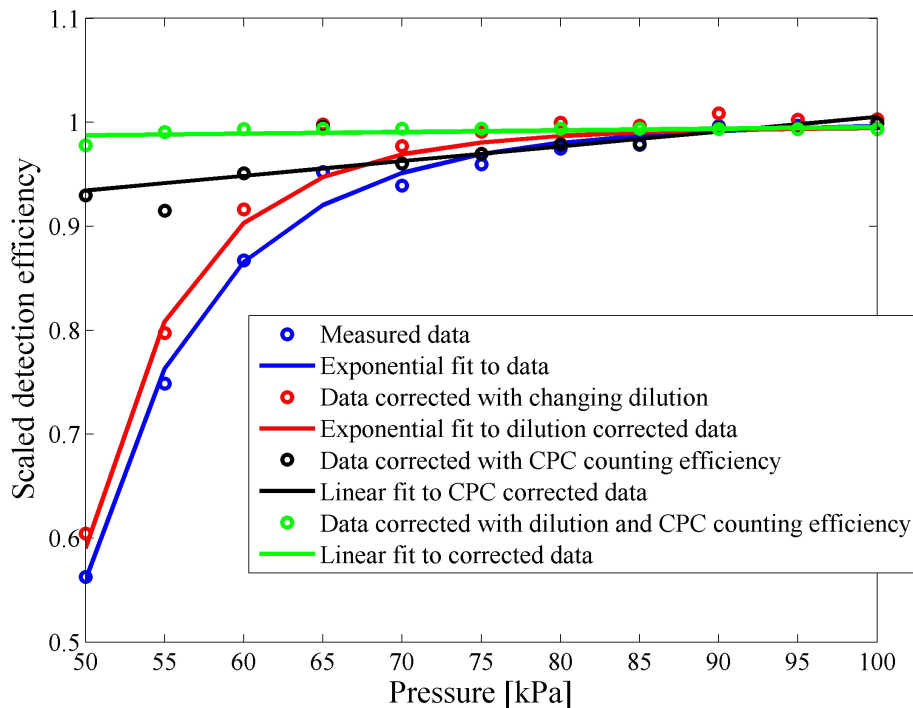


Figure 5. PSM detection efficiency measured at different pressures for 50 nm ammonium sulfate aerosol. Curves have been normalized to unity to separate the two corrections needed: changing dilution and lowering CPC counting efficiency with pressure.

Operation of Airmodus PSM

J. Kangasluoma et al.

Title Page	
Abstract	Introduction
Conclusions	References
Tables	Figures
◀	▶
◀	▶
Back	Close
Full Screen / Esc	
Printer-friendly Version	
Interactive Discussion	



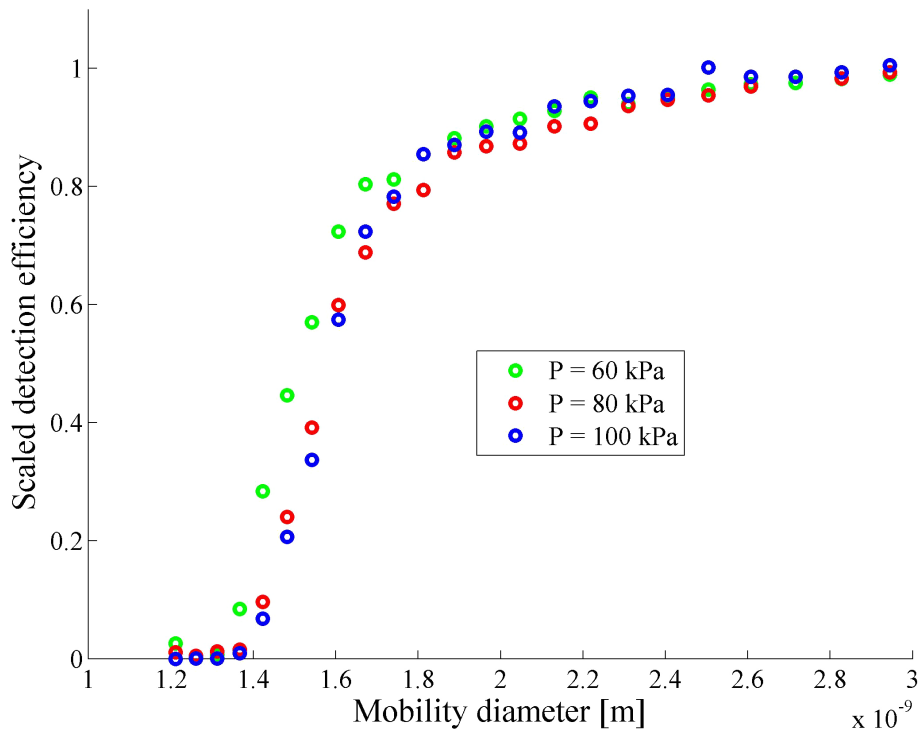


Figure 6. Measured PSM cut-offs at 60, 80 and 100 kPa pressure. The cut-off diameter stays almost constant.

Operation of Airmodus PSM

J. Kangasluoma et al.

Title Page	
Abstract	Introduction
Conclusions	References
Tables	Figures
◀	▶
◀	▶
Back	Close
Full Screen / Esc	
Printer-friendly Version	
Interactive Discussion	



**Operation of
Airmodus PSM**

J. Kangasluoma et al.

Title Page

Abstract

Introduction

Conclusions

References

Tables

Figures



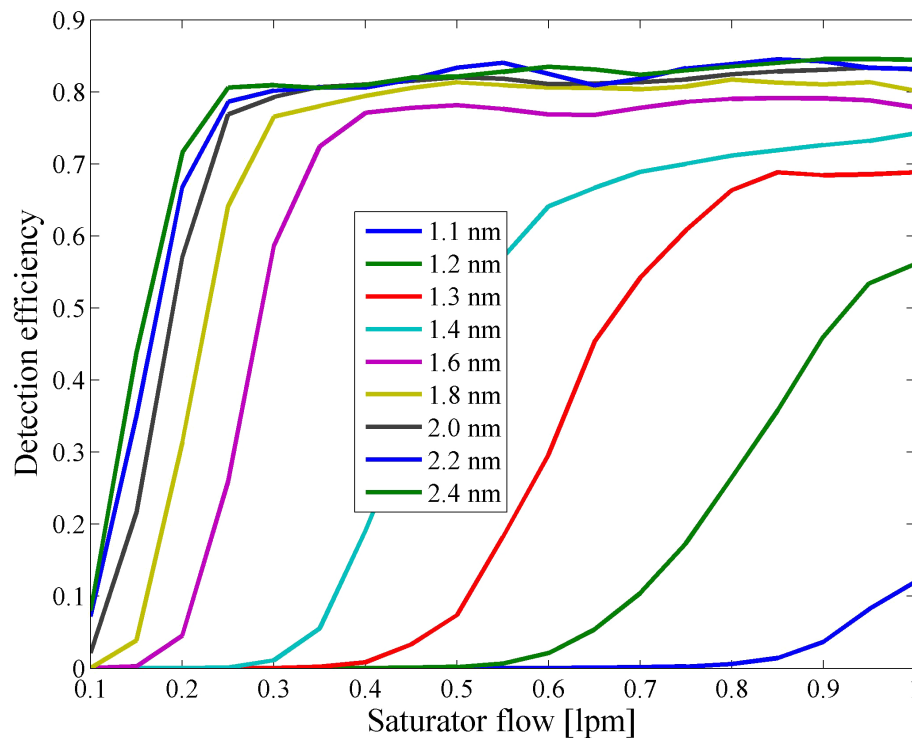
Back

Close

Full Screen / Esc

Printer-friendly Version

Interactive Discussion

**Figure 8.** The PSM calibrated as a laminar type CPC.

Operation of Airmodus PSM

J. Kangasluoma et al.

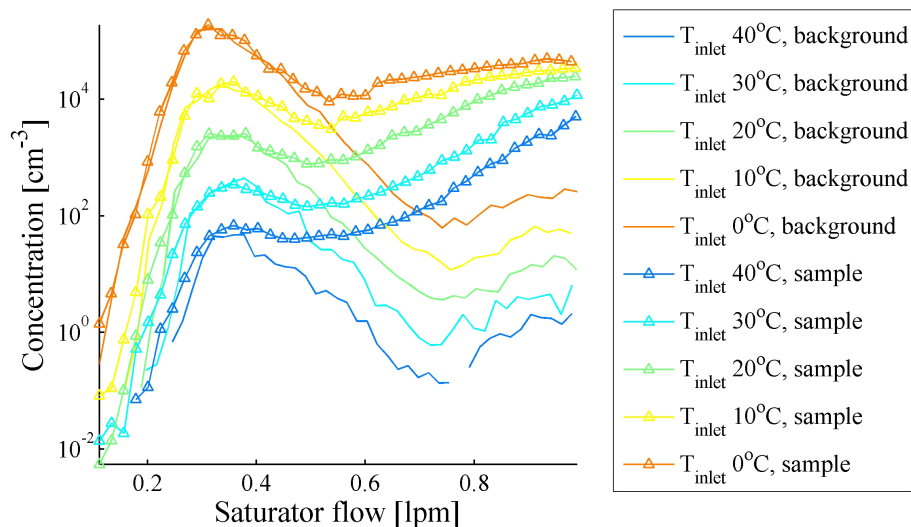


Figure 9. THABr monomer and background concentration measured as a function of saturator flow. Triangles present the background concentration and squares the concentration when THABr monomer is going in. Peak around 0.3 L min⁻¹ saturator flow is mixing type activation while at 1 L min⁻¹ laminar mode activation.

Title Page

Abstract

Introduction

Conclusions

References

Tables

Figures

◀

▶

◀

▶

Back

Close

Full Screen / Esc

Printer-friendly Version

Interactive Discussion



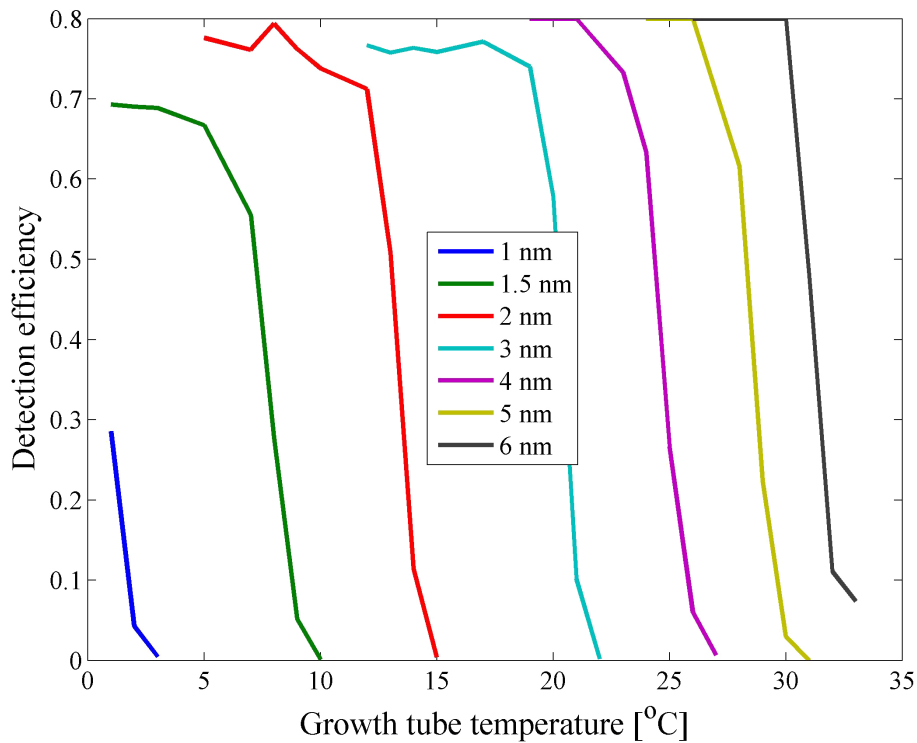


Figure 10. PSM calibration for particles of different sizes with varying growth tube temperature.

Operation of Airmodus PSM

J. Kangasluoma et al.

Title Page

Abstract Introduction

Conclusions References

Tables Figures

◀ ▶

◀ ▶

Back Close

Full Screen / Esc

Printer-friendly Version

Interactive Discussion



Operation of
Airmodus PSM

J. Kangasluoma et al.

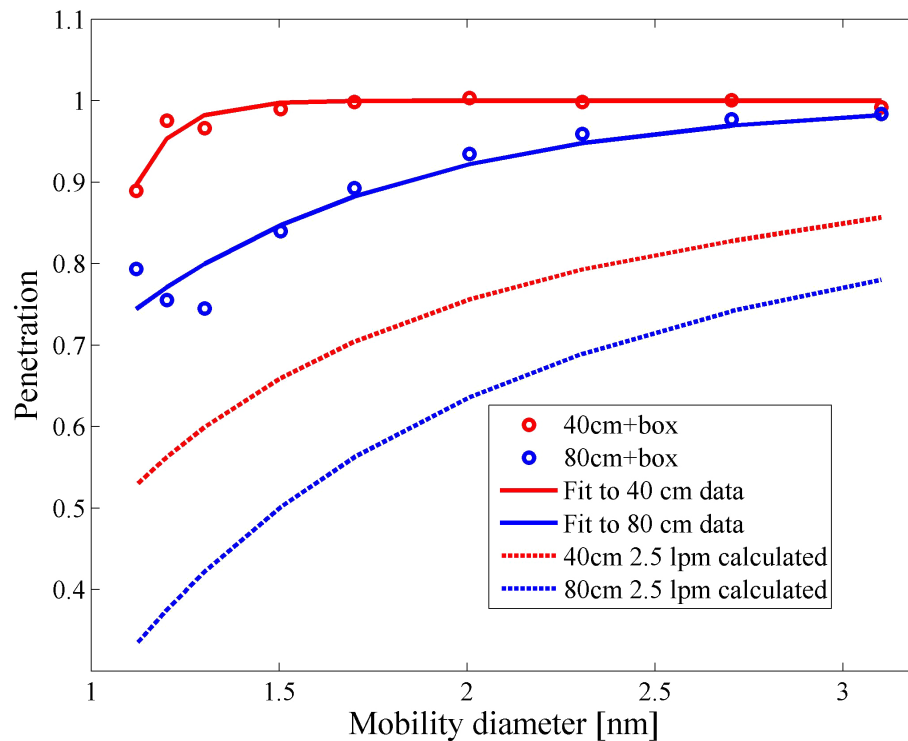


Figure 11. Penetration of negative tungsten oxide through the sampling line. With 40 cm inlet tube the penetration is close to unity for all sizes.

[Title Page](#)[Abstract](#)[Introduction](#)[Conclusions](#)[References](#)[Tables](#)[Figures](#)[◀](#)[▶](#)[◀](#)[▶](#)[Back](#)[Close](#)[Full Screen / Esc](#)[Printer-friendly Version](#)[Interactive Discussion](#)

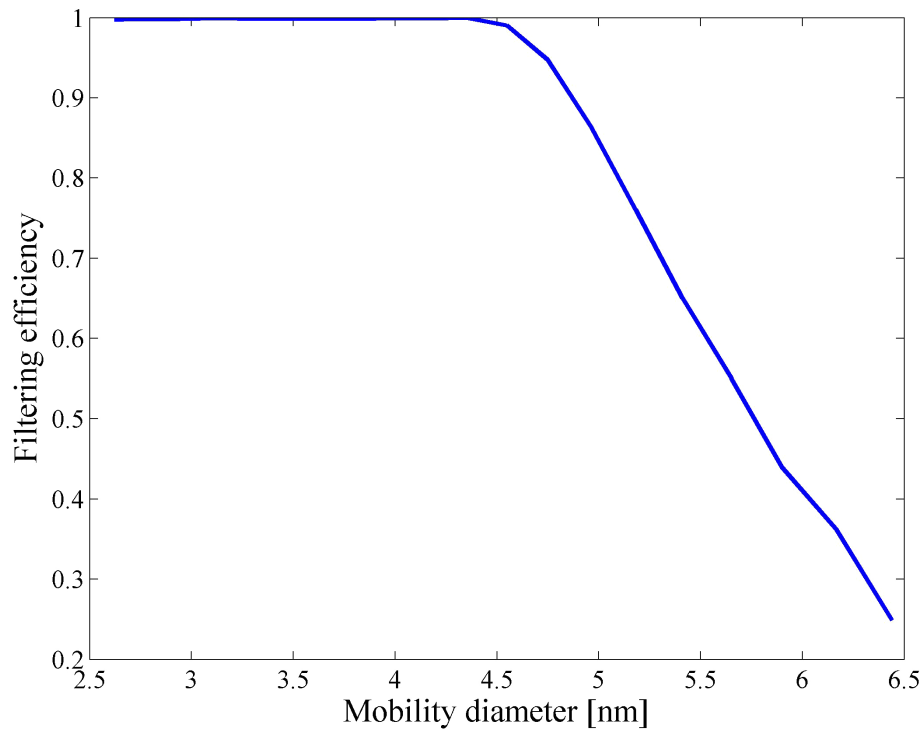


Figure 12. Ion filtering efficiency for the sampling inlet.

Operation of Airmodus PSM

J. Kangasluoma et al.

Title Page	
Abstract	Introduction
Conclusions	References
Tables	Figures
◀	▶
◀	▶
Back	Close
Full Screen / Esc	
Printer-friendly Version	
Interactive Discussion	

